

Long Term Changes and Trends in the Atmosphere

Volume II

Editor

GUFRAN BEIG

***Stratospheric Temperature Changes:
Observations and Model Simulations***

V. Ramaswamy

*NOAA/Geophysical Fluid Dynamics Laboratory,
Princeton University, Princeton, NJ 08542, USA*

(e-mail: vr@gfdl.gov)



NEW AGE INTERNATIONAL (P) LIMITED, PUBLISHERS

New Delhi • Bangalore • Calcutta • Chennai • Guwahati
Hyderabad • Lucknow • Mumbai

Stratospheric Temperature Changes: Observations and Model Simulations

V. Ramaswamy

NOAA/Geophysical Fluid Dynamics Laboratory,

Princeton University, Princeton, NJ 08542, USA

(e-mail: vr@gfdl.gov)

Abstract

Observations of stratospheric temperatures over the past three decades indicate a general cooling of the global lower stratosphere, and a pronounced cooling of the upper and middle stratosphere. This paper examines the long-term trends as inferred from a variety of available observations. Model simulations of temperature response due to changes in concentrations of radiatively active species are also analyzed. A comparative evaluation of the model simulations with observations reveals the extent to which the global-mean and zonal-mean lower stratosphere temperature trends can be attributed to trace gas changes.

Introduction

For at least a decade now, the investigation of trends in stratospheric temperatures has been recognized as an integral component of ozone change investigations (e.g. WMO reports since early 1980s). A comprehensive international scientific assessment of stratospheric temperature changes was undertaken in WMO (1990a). Since the WMO (1990a) assessment, there has been an ever-growing impetus for observational and model investigations of the stratospheric temperature trends, as evidenced, for example, in successive WMO assessments. This has occurred owing to the secular increases in greenhouse gases and the now well-documented global and seasonal losses of stratospheric ozone, both of which have a substantial impact on the stratospheric radiative-dynamical equilibrium. The availability of various temperature observations and the ever-increasing length of the data record have also been encouraging factors. In addition, models have progressively

acquired the capability to perform more realistic simulations of the stratosphere. This has provided a motivation for comparing model results with observations, and thereby searching for causal explanation/s of the observed trends. The assessment of stratospheric temperature trends is now regarded as a high priority in climate change research inasmuch as it has been shown to be a key entity in the detection and attribution of the observed vertical profile of temperature changes in the Earth's atmosphere (Santer *et al.*, 1996).

An excellent perspective of the evolution in the state-of-the-science of the stratospheric temperature trends can be found in the WMO Ozone assessment reports—WMO (1986, 1990a, 1990b, 1992, 1995 and 1999). In addition to the WMO assessment activities during the 1990s, an important development in mid-1990s was the initiative by the World Climate Research Program's (WCRP) Stratospheric Processes and their Role in Climate (SPARC) project. SPARC set up a Stratospheric Temperature Trends Assessment (STTA) group to focus on (i) bringing together all available data sets, examining the quality of the data and inter-comparing the resulting global stratospheric temperature trends; and (ii) employing model simulations in conjunction with the measurements to search for the causes of the observed trends, with an emphasis on the potential roles of the anthropogenic species.

In this paper, we cite first the observational platforms that provide insights into the long-term trends in stratospheric temperatures over the past 2–3 decades, followed by the trend estimates, and a discussion of the uncertainties. We follow this by discussions of the model investigations dealing with the impacts of observed changes in trace gas concentrations upon lower stratospheric temperatures. Subsequently, inferences regarding the possible cause/s and attribution of the observed temperature trends, particularly during the 1980s, appear followed by the concluding remarks. A detailed exposition of the material here appears in WMO (1999; Chapter 5).

Observations

The types of observational data available for investigation into stratospheric temperature trends are diverse. They differ in type of measurement, length of time period and space-time sampling. There have been several investigations of trends that have considered varying time spans with the different available data sets. In a major inter-comparison effort, the SPARC-STTA group brought together a variety of data sets, and have derived and inter-compared global stratospheric temperature trends. STTA selected two different time periods to examine the trends, 1979–1994 and ~1965–1994. The shorter period coincides with the period when severe global ozone losses have been detected; further, satellite observations began in ~1979. The second period is a longer one for which radiosonde (and a few rocketsonde) data sets are available.

The updated data sets made available to and employed by the SPARC-STTA for the analyses are shown (with the exception of the rocketsondes) in Table 1 along with their respective latitudes, altitudes and periods of coverage. Additionally, independent of the STTA activity, some investigations [Dunkerton *et al.* (1998), Keckhut *et al.* (1998), Komuro (1989), Golitsyn *et al.* (1996) and Lysenko *et al.* (1997)] have analyzed trends from rocketsonde observations made at a few geographical locations and over specific time periods (*see* Table 2). We utilize these datasets in the presentations to follow. It is convenient to group the currently known datasets as follows:

Ground-based instruments: radiosonde, rocketsonde, and lidar;

Satellite instruments: microwave and infrared sounders; and

Analyses: employing data from one or both of the above instrument types, without/ with a numerical model.

The datasets indicated in Table 1 are a collection of monthly-mean, zonal-mean temperature time series. All but one of these datasets cover the years 1979–1994, and some extend further back in time. The pressure-altitude levels of the datasets vary, but overall they cover the range 100 to 0.4 hPa (approximately 16–55 km). Most datasets provide temperatures at specific pressure levels, but some provide data as mean temperatures representative of various pressure-layers. The records from radiosondes, rocketsondes, lidar and satellite (MSU and SSU) are virtually independent of each other. General characteristics of the different datasets are discussed in WMO (1990a, 1990b, 1999).

Radiosonde

Radiosonde data for the stratosphere are available dating back to approximately the late 1950s. Although the sonde data do not cover the entire globe, there have been several well-documented efforts to use varied techniques in order to obtain the temperatures over the entire northern hemisphere or the global domains. In the stratosphere, the sonde data cover primarily the lower stratospheric region (i.e. pressure levels exceeding 30 hPa). The geographical coverage is quite reasonable in the Northern Hemisphere (particularly midlatitudes) but is poor in the extremely high latitudes and tropics, and is seriously deficient in the Southern Hemisphere (Oort and Liu, 1993). The various radiosonde datasets, along with key references that describe the methodology, are: “Berlin” (Labitzke and van Loon, 1995), “Angell” (1988), “Oort” (Oort and Liu, 1993), UK “RAOB” (Parker *et al.*, 1997), and “Russia” (Koshelkov and Zakharov, 1998).

Table 1 Zonal temperature time series made available to and considered by SPARC-STTA. Angell, Oort, Russia, Raob and Berlin are different radiosonde datasets. MSU and Nash are satellite instruments while lidar data is from OHP (France). CPC, Reanal, UKMO/ SSUANAL and GSFC are analyzed datasets. For the MSU and Nash satellite data, the approximate peak levels 'sensed' are listed. References to earlier versions of the datasets are also listed.

<i>Dataset</i>	<i>Period</i>	<i>Location</i>	<i>Monthly</i>	<i>Levels (hPa)</i>
Angell	1958–1994	8 bands	3-Monthly	100–50
[Angell, 1988]		4 bands	3-Monthly	50, 30, 20, 10
Oort	1958–1989	85S–85N	Monthly	100, 50
[Oort and Liu, 1993]				
Russia	1959–1994	70N, 80N	Monthly	100
	1961–1994	70N, 80N	Monthly	50
[Koshelkov and Zakharov, 1998]				
UK Raob (or Raob)	1961–1994	87.5S–87.5N	Monthly	100, 50, 30, 20
Berlin	1965–1994	10–90N	Monthly	100, 50, 30
Lidar	1979–1994	44N, 6E	Monthly	10, 5, 2, 1, 0.4
[Hauchecorne <i>et al.</i> , 1991]				
MSU	1979–1994	85S–85N	Monthly	90
[Spencer and Christy, 1993]				
Nash	1979–1994	75S–75N	Monthly	50, 20, 15, 6, 5, 2, 1.5, 0.5
[Nash and Forrester, 1986]				
CPC	1979–1994	85S–85N	Monthly	70, 50, 30, 10, 5, 2, 1
[Gelman <i>et al.</i> , 1994]	1964–1978	20N–85N	Monthly	50, 30, 10
Reanal	1979–1994	85S–85N	Monthly	100, 70, 50, 30, 10
[Kalnay <i>et al.</i> , 1996]				
GSFC	1979–1994	90S–90N	Monthly	100, 70, 50, 30, 20
[Schubert <i>et al.</i> , 1993]				
UKMO/SSUANAL	1979–1994	90S–90N	Monthly	50, 20, 10, 5, 2, 1
[Bailey <i>et al.</i> , 1993]				

Table 2 *Rocketsonde locations and periods of coverage [based on Dunkerton et al., 1998; Golitsyn et al., 1996; Keckhut et al., 1998; Kokin and Lysenko, 1994; Lysenko et al., 1997; and Komuro, 1989 (updated)].*

<i>Station</i>	<i>Latitude-Longitude</i>	<i>Period</i>
Heiss Island	81°N; 58°E	1964–1994
Volgograd	49°N; 44°E	1965–1994
Balkhash	47°N; 75°E	1973–1992
Ryori	39°N; 141.5°E	1970–Present
Wallops Island	37.5°N; 76°W	1965–1990
Point Mugu	34°N; 119°W	1965–1991
Cape Kennedy	28°N; 80°W	1965–1993
Barking Sands	22°N; 160°W	1969–1991
Antigua	17°N; 61°W	1969–1991
Thumba	08°N; 77°E	1971–1993
Kwajalein	09°N; 167°E	1969–1990
Ascension Island	08°S; 14°W	1965–1993
Molodezhnaya	68°S; 46°E	1969–1994

Rocket and Lidar

Rocket and lidar data cover the altitude range from about the middle into the upper stratosphere and mesosphere. Rocketsonde data are available through the early 1990s from some locations but the activity appears to be virtually terminated except in Japan (*see* Table 2). The lidar measurement, just like the rocketsondes, has a fine vertical resolution. Lidar measurements of stratospheric temperatures are available since 1979 from the Haute Provence Observatory (OHP) in southern France (44°N, 6°E). Specifically, the “lidar” (Table 1) temperatures observed at altitudes of 30 to 90 km are obtained from two lidar stations, with data interpolated to pressure levels (Keckhut *et al.*, 1995). Several other lidar sites have initiated operations and could potentially contribute in future temperature trends assessments.

MSU and SSU Satellites

Satellite instruments that remotely sense stratospheric temperatures have become available since ~1979 (Table 1). An important attribute of the satellites is their global coverage. The satellite instruments fall into two categories—remotely sensing in the microwave (Spencer and Christy, 1993) and thermal infrared (Nash and Forrester, 1986) wavelengths. In contrast to the ground-based measurements, e.g. the radiosonde, which perform measurements at specific pressure levels, the available satellite sensors sense the signal from a wide range in altitude.

The nadir satellite instruments ‘sense’ the emission originating from a layer of the atmosphere typically 10–15 km thick. The “MSU” Channel 4 dataset derives from the lower stratosphere channel (~150–50 hPa) of the Microwave Sounding Unit on NOAA polar operational satellites. The “Nash” dataset consists of brightness temperatures from observed (25, 26 and 27) and derived (47X, 36X, 35X, 26X and 15X) channels of the Stratospheric Sounding Unit (SSU) and HIRS-2 instruments on these same satellites (*see* WMO, 1990a).

One complication with satellite data is the discontinuity in the time series owing to the measurements being made by different satellites monitoring the stratosphere since 1979. Adjustments have been made in the “Nash” channel data to compensate for radiometric differences, tidal differences between spacecraft, long-term drift in the local time of measurements, and spectroscopic drift in channels 26 and 27. Adjustments have also been made to MSU data (e.g. Christy *et al.*, 1995). The MSU record has been discussed in WMO (1995).

Analyzed Datasets

There are a number of datasets that involve some kind of analyses of the observations. They employ one or more types of observed data, together with the use of some mathematical technique and/ or a general circulation model for data assimilation and analysis, to construct the global time series of the temperatures. They are, in essence, more a derived dataset than the satellite- or the ground-based ones. The “CPC” (Climate Prediction Center, formerly Climate Analyses Center or “CAC”) and “UKMO/SSUANAL” stratospheric analyses (Table 1) do not involve any numerical atmospheric circulation model. The “CPC” northern hemisphere 70, 50, 30 and 10 hPa analyses use radiosonde data. Both the “CPC” and “UKMO/SSUANAL” analyses (*see* also Bailey *et al.*, 1993) use TOVS (TIROS Operational Vertical Soundings) temperatures, which incorporate data from the SSU, HIRS-2, and MSU on the NOAA polar orbiting satellites. Although mentioned here for completeness’ sake, the analyses below ignore the “UKMO/SSUANAL” data. The “Reanal” (*viz.*, the US National Centers for Environmental Prediction or NCEP reanalyzed) and the “GSFC” (NASA) datasets are derived using numerical atmospheric general circulation models as part of the respective data assimilation systems. These analysis projects provide synoptic meteorological data extending over many years using an unchanged assimilation system. In general, analyzed datasets are dependent on the quality of the data sources such that a spurious trend in a data source could be inadvertently incorporated in the assimilation. In addition, gaps in the data pose severe constraints. Also, analyses do not necessarily account for longer-term calibration related problems in the data, and they may not contain adjustments for satellite data discontinuity.

Trends

As examples of the observed trend estimates, we examine the changes in the lower stratosphere (50–100 hPa) temperatures, and the vertical profile of temperature change from the lower to middle/ upper stratosphere (100 to 1 hPa).

Lower Stratosphere

Figure 1 illustrates the decadal trends for the different datasets over the 1979–1994 period, as evaluated by the SPARC-STTA. For the non-satellite datasets, the trends at 50 and 100 hPa are illustrated in panels (a) and (b), respectively; panel (c) illustrates the satellite-derived trends. [The Oort data, which have been used widely (e.g. Hansen *et al.*, 1995; Santer *et al.*, 1996), are not included in this plot because they span a shorter period of time (1979–1989) than the other datasets.]. In the case of the MSU and Nash (SSU 15X) satellite data, the trend illustrated in panel (c) is indicative of a response function that spans a wide range in altitude, e.g. for MSU, about half of the signal originates from the upper troposphere at the low latitudes. Because of this, caution must be exercised in comparing the magnitudes of the non-satellite trends in panels (a) and (b) with those for the satellite in panel (c). This aspect could explain, in part, the lesser cooling obtained by the satellites relative to radiosondes in the tropical regions; however, this argument is contingent upon the trends in the tropical upper troposphere. From an analysis of radiosonde data, Parker *et al.* (1997) find that the transition height between tropospheric warming and cooling to occur at about 200 hPa, when comparing the period 1987–1996 with 1965–1974; this would indicate that part of the MSU weighting function would be sampling altitudes at which some warming has occurred. [For a further perspective on trends in upper troposphere, see Hansen *et al.*, 1997b; Santer *et al.*, 1998]. However, a more satisfactory analysis would require radiosonde based trends for the same period as the MSU data. The MSU indicates less cooling than Nash in the tropics. One reason for this could be that the Nash peak signal originates from a slightly higher altitude than MSU; again, though, the extent of the cooling/ warming trend in the upper troposphere needs to be considered for a full explanation. The results are statistically insignificant in almost all of the datasets at the low latitudes (WMO, 1999). This could be in part due to the variable quality of the tropical data. It is conceivable that the radiosonde trends are significant over selected regions where the data are reliable over long time periods, but that the significance is destroyed when reliable and unreliable data are combined to get a zonal mean.

All datasets indicate a cooling of the entire northern hemisphere and the entire low and mid latitude southern hemisphere at the 50 hPa level over this period. At the 100 hPa level, there is a cooling over most of the northern and southern latitudes. The midlatitude (30–60N) trends in the northern hemisphere exhibit a

statistically significant cooling at both 50 and 100 hPa levels (WMO, 1999), with the magnitude in this region being $\sim 0.5\text{--}1\text{K/decade}$. This feature is found in satellite data as well. The similarity of the magnitude and significance in the mid-northern hemisphere latitudes from the different datasets is particularly encouraging and suggests a robust trend result for this time period. The trends in the southern hemisphere midlatitudes ($\sim 15\text{--}45\text{S}$) range up to $\sim 0.5\text{--}1\text{K/decade}$, but are generally statistically insignificant over most of the area in almost all datasets, except Reanal (WMO, 1999). Note that the southern hemisphere radiosonde data has more uncertainties owing to fewer observing stations and data homogeneity problems. The non-satellite data indicate a warming at 50 hPa but a cooling at 100 hPa at the high southern latitudes, while the satellites indicate a cooling trend. Thus, as for the tropical trends, satellite-radiosonde intercomparisons in this region have to consider carefully the variation of the trends with altitude. The lack of statistically significant trends in the southern high latitudes need not imply that significant trends do not occur during particular seasons (e.g. Antarctic spring time). The high northern latitudes indicate a strong cooling (1K/decade or more) in the 50 hPa, 100 hPa and satellite datasets. However, no trends are significant poleward of $\sim 70\text{N}$ owing to the large interannual variability there. There is a general consistency of the analyzed datasets (CPC, GSFC, Reanal) with trends derived directly from the instrumental data. Considering all datasets, the global lower stratospheric cooling trend over the 1979–1994 period is estimated to be $\sim 0.6\text{ K/decade}$. The 50–100 hPa cooling is consistent with earlier WMO results based on shorter records (1988 (e.g. Figure 6.17); 1990 (e.g. Figure 2.4–5)).

Figure 2 shows the annual-mean trend over 1966–1994 at 50 hPa and comprises only the radiosonde record. Note that the Oort time series extends only until 1988. The cooling trends in the northern high latitudes, and in several other latitude belts, are less strong in the radio sonde datasets when the longer period is considered. The cooling trend in the $30\text{--}60\text{N}$ belt is about 0.3K/decade . The strong cooling trend in the Oort data in the high southern latitudes is consistent with Oort and Liu (1993), Parker *et al.* (1997) and the Angell data. In the southern hemisphere, the two global radiosonde datasets indicate a significant cooling over broad belts in the low and midlatitudes, with the Oort data exhibiting this feature at even the higher latitudes. The Oort global-mean trend is -0.33 K/decade over the 1966–1989 period. In the northern hemisphere, again, the midlatitude regions stand out in terms of the significance of the estimated trends (WMO, 1999). Latitudes as low as $10\text{--}20$ degrees exhibit significant trends over the longer period considered.

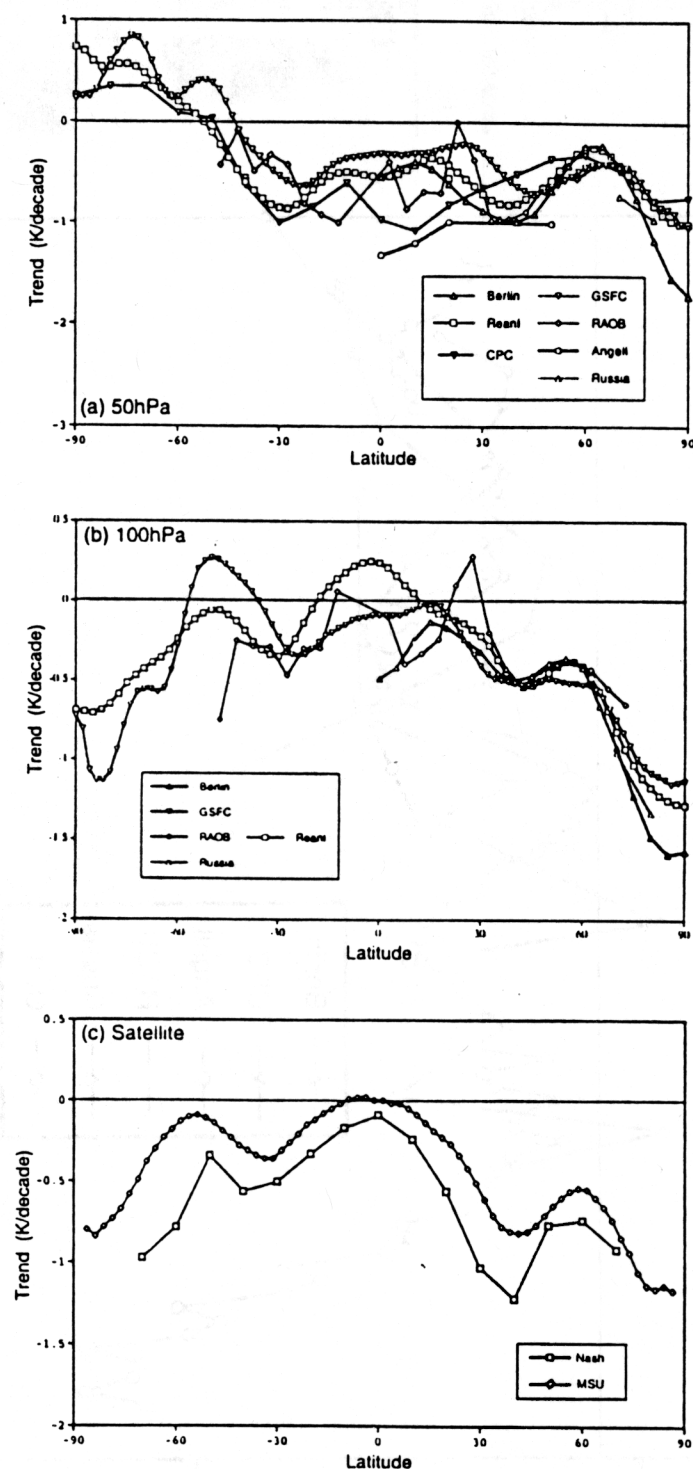


Fig. 1 Zonal-mean decadal temperature trends for the 1979–1994 period, as obtained from different datasets. These consist of radiosonde (Angell, Berlin, UKMO/ Raob and Russia) and satellite observations (MSU and Nash), and analyses datasets (CPC, GSFC and Reanal). (a) denotes 50 hPa trends, (b) denotes 100 hPa trends, and (c) denotes trends observed by the satellites for the altitude range 'sensed' which includes the lower stratosphere. [Data courtesy of SPARC-Stratospheric Temperature Trends Assessment project].

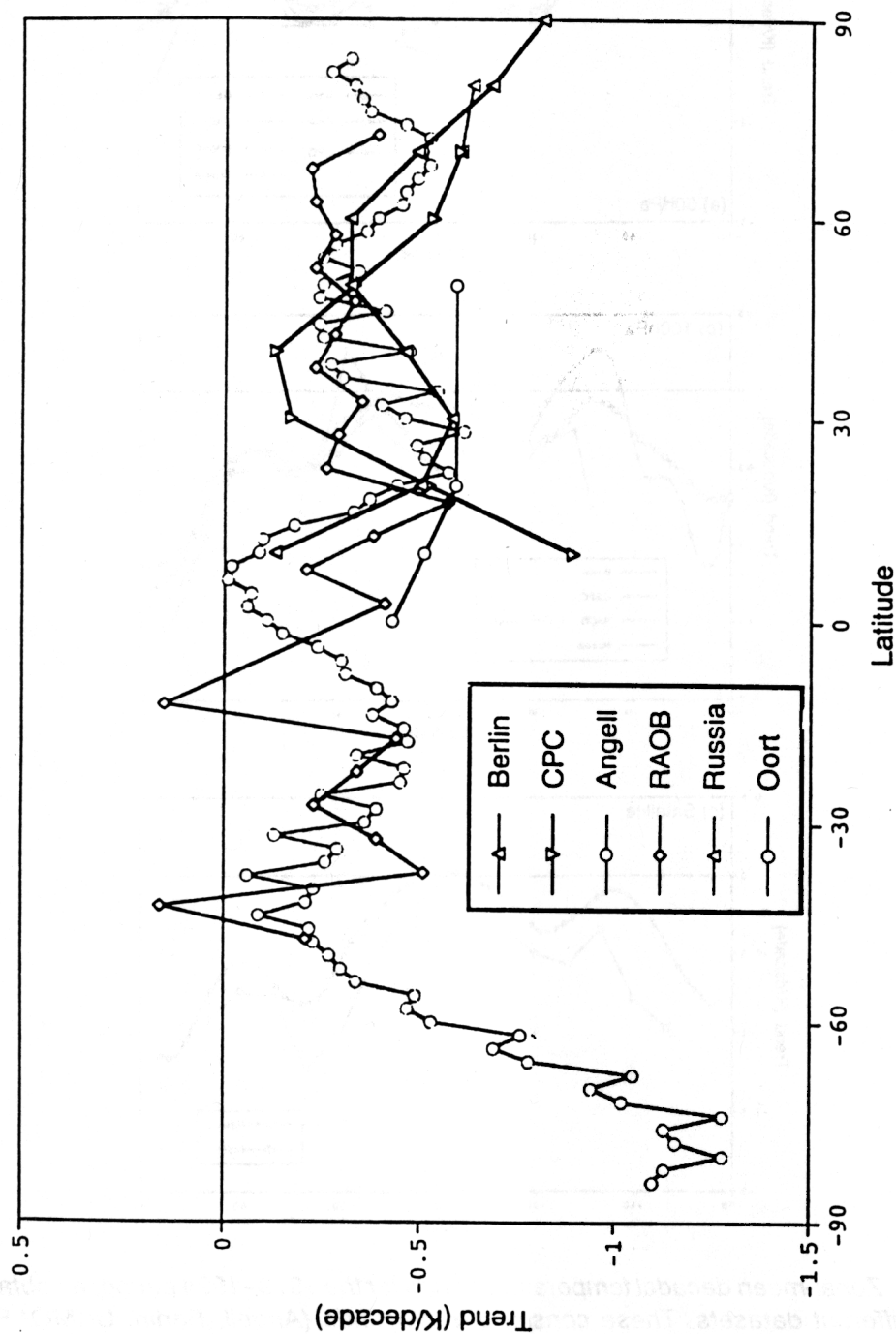


Fig. 2 Zonal-mean decadal temperature trends at 50 hPa over the 1966–1994 period from different datasets. [Data courtesy of SPARC-Stratospheric Temperature Trends Assessment project].

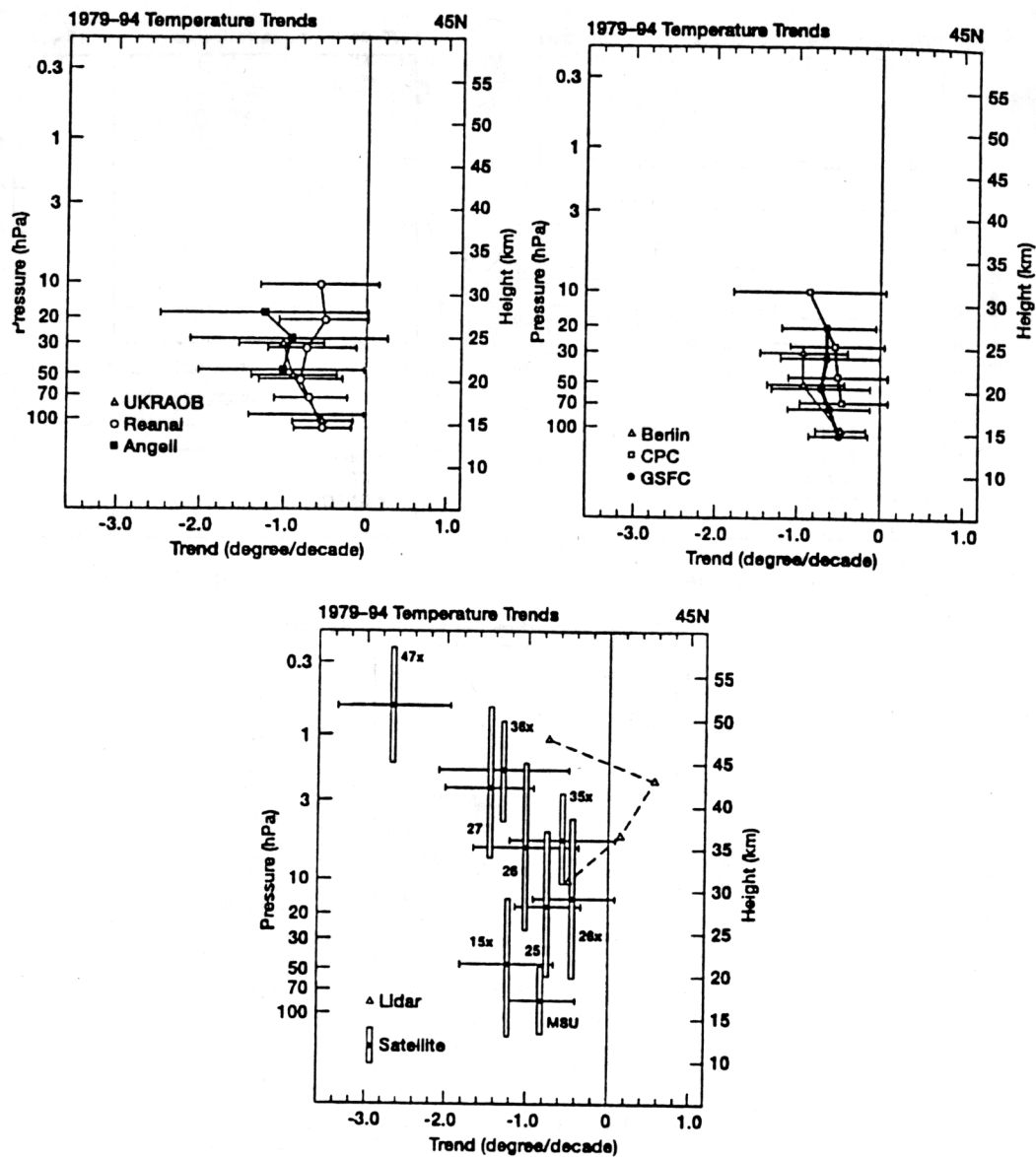


Fig. 3 Vertical profile of the zonal, annual-mean decadal stratospheric temperature trend over the 1979–1994 period at 45N from different datasets (Table 1) for the 1979–1994 period. Horizontal bars denote statistical significance at the 2-sigma level while vertical bars denote the approximate altitude range 'sensed' by the MSU, and by the different SSU satellite channels. [Data courtesy of SPARC-Stratospheric Temperature Trends Assessment project].

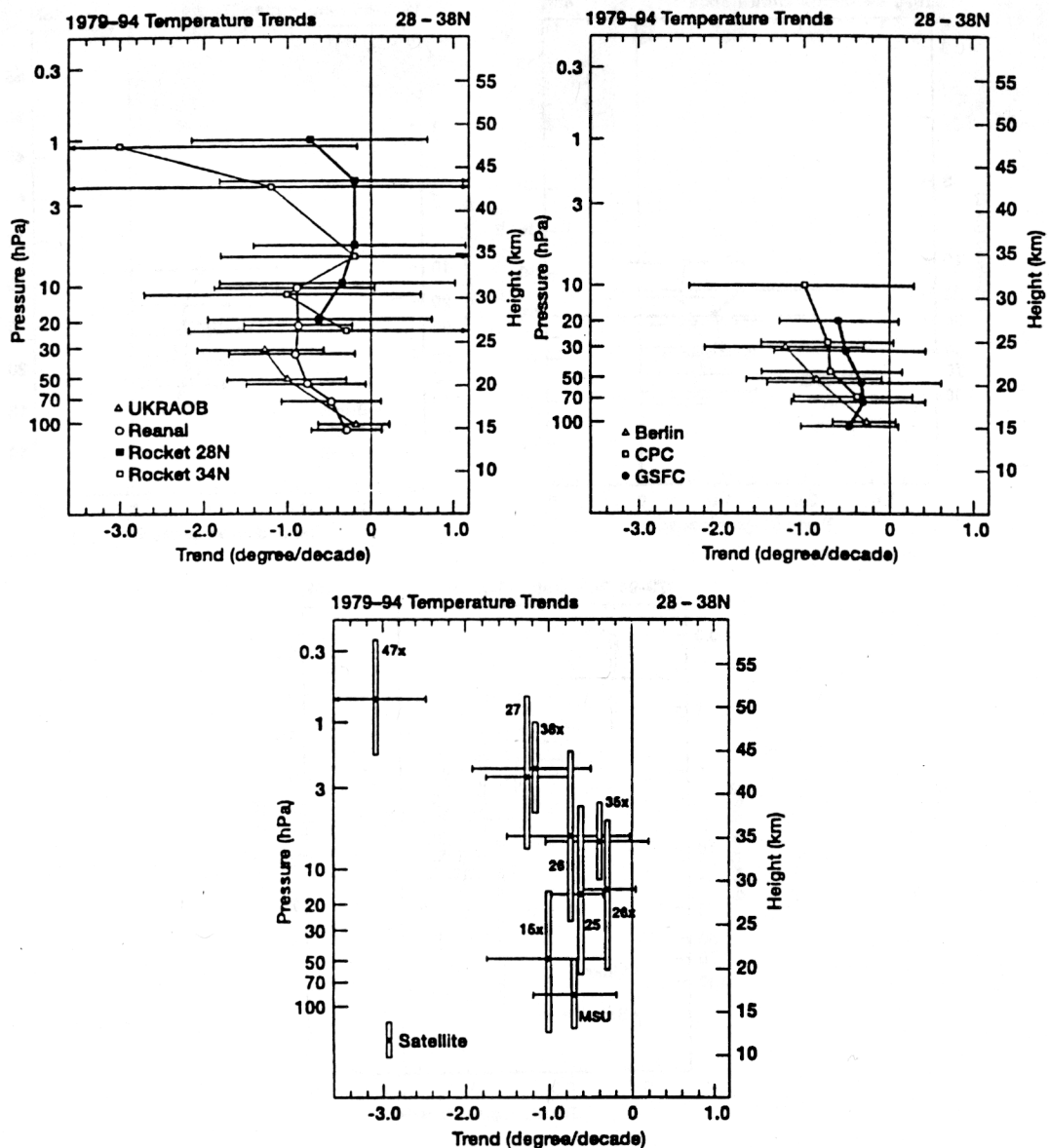


Fig. 4 Vertical profile of the zonal, annual-mean decadal stratospheric temperature trend over the 1979–1994 period at 28–38°N from different datasets (Tables 1 and 2). Horizontal bars denote statistical significance at the 2-sigma level while vertical bars denote the approximate altitude range 'sensed' by the MSU and by the different SSU satellite channels. [Data courtesy of SPARC-Stratospheric Temperature Trends Assessment project].

Vertical Profile

Figure 3 compares the vertical pattern of temperature trend at 45N obtained from different datasets for the 1979–1994 period. There is a broad agreement in the cooling at the lower stratospheric altitudes, reiterating Figure 1. The vertical pattern of the trends from the various data are also in qualitative agreement, except for the lidar data (which, in any case, is not statistically significant over that height range). Generally speaking, there is an approximately uniform cooling of about 0.75 K/decade between ~80 and 5 hPa (~18–35 km), followed by increasing cooling with height (e.g. ~2.5 K/decade at 1 hPa {~50 km}). The “analyses” datasets, examined here for $p > 10$ hPa, are in approximate agreement with the instrument-based data. The vertical profile of cooling, and especially the large upper stratospheric cooling, are consistent with the global plots in WMO (1990a, Fig. 6.17; 1990b, Fig. 2.4–5) constructed from shorter data records.

Figure 4 compares the vertical profiles of trends over the 1979–1994 period from various datasets at ~30N, including the rocket stations at 28N (Cape Kennedy) and 34N (Point Mugu). As at 45N (Figure 3), almost all the datasets agree in the sign (though not in the precise magnitude) of temperature change below about 20 hPa (~27 km). Above 10 hPa (~30 km), both satellite and rocket trends yield increasing cooling with altitude, with a smaller value at the 28N rocket site. At 1 hPa, there is considerable divergence in the magnitudes of the two rocket trends. Because the rocket trends are derived from time series at individual locations, this may explain their greater uncertainty relative to the zonal-mean satellite trends. In a general sense, the vertical profile of the trend follows a pattern similar to that at 45N (Figure 3).

Uncertainties in Trends

Determining stratospheric temperature trends from long-term observations is complicated by the presence of additional, non-trend variability in the data. Two types of phenomena contribute to the uncertainty in trend estimates. The first is random variability that is internally generated within the atmosphere and that is not trend-like in nature. Major sources of such variability include: the (quasi-) periodic signals associated with the annual cycle, the quasi-biennial oscillation, the solar cycle, and the El Niño-Southern Oscillation (ENSO). In addition, stratospheric temperatures vary in response to episodic injections of volcanic aerosols. To first approximation, these atmospheric phenomena have negligible effects on the long-term temperature trend because they are periodic or of relatively short duration. Nevertheless, because current data records are only a few decades long, at most, these phenomena may appear to enhance or reduce an underlying trend. At a minimum, the additional temperature variability associated with these signals reduces the statistical confidence with which long-term trends can be

identified. While periodic signals can be removed, the effects of sporadic events are more difficult to model and remove. Furthermore, there may be long-term trends in these cycles and forcings that confound the analysis. A second source of uncertainty is due to spurious signals in the time series that are due to changes in methods of observation rather than to changes in the atmosphere. The problem of detecting temperature trends in the presence of changes in the bias characteristics of the observations is receiving increased attention (Christy, 1995; Santer *et al.*, 1998). It seems likely that over the next few years better methods will be employed to quantify and reduce the uncertainty in stratospheric temperature trend estimates attributable to these spurious signals.

Radiosonde Data

Although most radiosonde analyses show cooling of the lower stratosphere in recent decades, it is important to recognize that they all rely on subsets of the same basic dataset, the global observing system upper-air network. This network is fundamentally a meteorological one, not a climate monitoring network, not a reference network for satellite observations, and not a network for detection of stratospheric change. Whatever difficulties plague the radiosonde network when it is employed for temperature trends analysis will affect all analyses that use those data.

The radiosonde network is predominantly a northern hemisphere, midlatitude, land network. About half the stations are in the 30–60N latitude band, and less than 20% are in the southern hemisphere (Oort and Liu, 1993). Moreover, the uneven distribution of stations is worse for stratospheric data than for the lower troposphere, because low latitude and southern hemisphere soundings have a higher probability of taking only one observation daily (other stations make two, and many formerly made four), and because the soundings more often terminate at lower altitudes (Oort and Liu, 1993). Estimates of layer-mean trends, and comparisons of trends at different levels, are less meaningful when data at the top of the layer are fewer than at the bottom.

Analyses of SSU Data

The stratospheric temperature analyses from CPC (NCEP) are an operational product, derived using a combination of satellite and radiosonde temperature measurements. Radiosonde data contribute to the analyses in the NH over the 70–10 hPa levels; satellite data alone are used in the tropics and SH, and over the entire globe above 10 hPa (Gelman *et al.*, 1986). The satellite temperature retrievals are from the TIROS Operational Vertical Sounder (TOVS), which have been operational since late 1978. A series of TOVS instruments (includes MSU and SSU) have been put into orbit aboard a succession of operational satellites; these instruments do not yield identical radiance measurements for a variety of

reasons, and derived temperatures may change substantially when a new instrument is introduced (Nash and Forrester, 1986). Finger *et al.* (1993) have found systematic biases in the upper stratosphere. Further, these biases change with the introduction of new operational satellites.

Satellite-Radiosonde Comparisons

A distinct advantage of the satellite instruments over in situ ones is their globally extensive coverage. This is tempered by the fact that the signals that they receive originate from a broad range of altitudes. This is in contrast to the specific altitudes of measurements in the case of the ground-based instruments located at specific sites. This feature of the satellite trends complicates the interpretation for any particular vertical region of the atmosphere and, more particularly hampers a rigorous comparison with, say, the radiosonde trends. As an example, consider the problem of the lower stratospheric temperature trends. The MSU's Channel 4 'senses' the entire extent of the lower part of the stratosphere, and even the upper troposphere at low latitudes. This poses problems in the precise intercomparison of presently available satellite-based trends with those from ground-based instruments. In the tropics, approximately half of the signal originates from the upper troposphere, leading to a potential misinterpretation of the actual lower stratospheric temperature trend based on MSU alone. This problem can become acute particularly if the tropical upper troposphere and lower stratosphere have temperature trends of opposite signs. A similar comment also applies to the interpretation of the stratosphere trends from SSU measurements. Further, because of the areal coverage of the low latitudes, the global-means from satellite data and those from the in situ instruments may be comparable only after appropriate adjustments are made for the differential sampling by the two kinds of instruments. Therefore, caution must be exercised in the interpretation of satellite-based trends vis-a-vis radiosonde and other ground-based instruments. Besides, satellite data interpretations also have to cope with problems involving temporal discontinuity, instrument calibration and orbit drift.

Rocket Data

The rocket data are very useful as they were the only observations of the 30–80 km. Region before the lidars started operating. However, determining quantitative trends from rocket data is complicated by both physical and measurement issues. A first difficulty with the rocket data is that there have been instrumental changes and the measurements come from different types of sensors (Arcasonde, datasonde, falling spheres). However, Dunkerton *et al.* (1998) have found that these changes were a less important source of error than previously suggested. The major source of error, and the origin of the observed spurious jumps, seems

to be due to the change of corrections of the data to take into account aerodynamic heating. Most of the earlier analyses did not take full account of the changes and of the spurious jumps in the data that ensued from the above-mentioned difficulties. These points have been considered in-depth by Keckhut *et al.* (1998) and Dunkerton *et al.* (1998), which resulted in a very limited number of US stations that could be used for determining trends. Yet another source of uncertainty is due to the different time of measurements, as the amplitude of tidal influence may not be negligible at these altitudes ($\pm 2\text{K}$ around 40–45 km. according to Gille *et al.* (1991) and Keckhut *et al.* (1996)).

Lidar Record

In a pure molecular atmosphere, temperature obtained from Rayleigh lidar are given in absolute value as a function of altitude without any need of external calibration. However, Rayleigh lidar measurements are affected by the presence of aerosols. After a major volcanic eruption, the stratospheric aerosols can reach altitudes up to nearly 40 km limiting thus the lower height range where the Rayleigh lidar temperature measurements can be made. An accuracy of 1% is easily attained, with a principal limit for ascertaining the significance of a trend being the length of the available data set. Using the actual measurements at the Haute Provence site, it was found that the establishment of a significance in the trend at the 95% level in the upper stratosphere required 20.5 years of data for summer and 35 years for winter trends. More years are required for the wintertime owing to the increased variability present in that season (Keckhut *et al.* 1995). Of course, the length of a period needed to establish statistical significance also depends on the amplitude of the signal.

Model Simulation

Concepts

In this section, we discuss results from model investigations that have analyzed the effects due to changes in trace species upon stratospheric temperatures. We examine the changes in the lower stratospheric region, and also mention the vertical profile of the modeled trends from the lower-to-upper stratosphere. Numerical models based on fundamental understanding of radiative, dynamical and chemical processes constitute essential tools for understanding the effects of specific mechanisms on temperature trends and variability in the stratosphere, and for interpreting observed temperature changes in terms of specific mechanisms. The numerical models used thus far have attempted to include, to varying degrees, the relevant components of the climate system which could influence stratospheric temperatures. The models also attempt to capture the important links between the stratosphere, troposphere and mesosphere.

It is well-recognized that the global, annual-mean thermal profile in the stratosphere represents a balance between solar radiative heating and longwave radiative heating and cooling, involving mainly ozone, carbon dioxide, water vapor, methane, nitrous oxide, halocarbons and aerosols (*see* Goody and Yung, Chapter 9 and references therein). In the context of the general global stratosphere, dynamical effects also become a factor in determining the thermal profile. Since the late 1950s, with increasing knowledge of trace species' concentration changes and their optical properties, numerical models have played a significant role in highlighting the potential roles of various constituents and the different mechanisms operating in the stratosphere. For example, WMO (1986; 1990a) concluded that changes in the concentrations of trace gases and aerosols could perturb substantially the radiative balance of the contemporary stratosphere and thereby affect its thermal state.

Early numerical models were developed as one-dimensional ones on the basis that the global, annual-mean stratosphere is in radiative equilibrium. This implies that, in the stratosphere, the thermal state determined is a balance between absorbed solar radiation and absorbed and emitted thermal infrared radiation. Together with the assumption of a radiative-convective equilibrium in the troposphere, this led to the so-called one-dimensional radiative-convective models (1D RCMs) which have been widely employed to study effects due to trace gas perturbations (WMO, 1986).

A variation of the RCMs is the so-called Fixed Dynamical Heating model or FDH model (Fels and Kaplan, 1975; Ramanathan and Dickinson, 1979; Fels *et al.*, 1980). The contemporary FDH models (e.g. WMO, 1992) hold the tropospheric temperature, humidity and cloud fields fixed and allow for changes in the stratospheric temperature in response to changes in radiatively active species. It is assumed that, in the unperturbed state, the radiative heating is exactly balanced by the dynamical heating at each height and latitude. If the concentration of a radiatively-active constituent is altered then the radiative heating field is altered. It is assumed that the dynamical heating remains unchanged, and that the temperature field adjusts in response to the perturbation. In turn, this alters the radiative heating field such that it again exactly balances the dynamical field.

The application of the RCM and FDH model concepts for understanding stratospheric temperature changes has evolved with time (*see* WMO: 1990a, 1992, 1995). Both types of models have been extensively used for gaining perspectives into the thermal effects due to the observed and projected changes in radiatively-active trace gases. These simple models, though, have important limitations. In particular, the FDH models can only predict temperature changes at any location due to constituent changes occurring there; i.e. the response is entirely localized within that particular stratospheric column. These simple models are nevertheless useful in yielding reasonable, first-order solutions of the problem.

There has been a steady progression from the simple RCMs and FDH models to the three-dimensional general circulation model (GCM; *see* WMO, 1986 for an early discussion of models used for studying the stratosphere) which seeks to represent the radiative-dynamical (and even chemical in some instances) interactions in their entirety. Such models have representations of radiative processes that may be less complete and accurate than in the 1D models, but provide the best means of mimicking the real atmosphere.

Effects due to Observed Ozone Depletion

Using the satellite-observed global lower stratospheric ozone losses over the ~1979–1991 period (i.e. just prior to the Pinatubo volcanic eruption), a comparison of the resulting radiative and radiative-dynamical solutions for the stratospheric temperature changes can be obtained. This is illustrated here by comparing (Figure 5) the results of the FDH and GCM simulations performed, respectively, by Ramaswamy *et al.* (1992) and (1996). This comparison enables a delineation of the role of radiative alone and dynamical influences on the temperature changes caused by the observed ozone depletion. The GCM result, like the FDH, indicates a cooling of the lower stratosphere, but there are distinct differences due to dynamical changes. In the mid-to-high southern latitudes, there is less cooling in the GCM. In the northern hemisphere, the mid-latitudes are less cold in the GCM, but the high latitudes are more so relative to the FDH result, again a consequence of the dynamical changes in the model. In the GCM, there is a cooling even in those regions where there are no ozone losses imposed, e.g. the lower stratosphere equatorward of 15 degrees. A warming occurs above the region of cooling, particularly noticeable in the southern hemisphere, similar to the results obtained by other GCM studies (Kiehl *et al.*, 1988; Mahlman *et al.*, 1994; Shindell *et al.*, 1998). The dynamical changes (*see* also Mahlman *et al.*, 1994) consist of an induced net rising motion in the tropics and a compressional heating of the middle stratosphere at the higher latitudes. The annual-mean response is statistically significant between ~13 and 21 km. in the ~20 to 50 degree latitude belt (Ramaswamy *et al.*, 1996). The changes at high latitudes (>60 degrees) fail the significance test because of large interannual variability in those regions. The warming above the lower stratospheric regions in both hemispheres is reasonably similar to observations (Randel, 1988; WMO, 1999).

Hansen *et al.*, (1993) show that the zonal-mean patterns of GCM-simulated lower stratospheric temperature change due to imposed ozone losses correspond well with observed changes. Ramaswamy *et al.* (1996) have compared the latitude-month trend pattern of the decadal (period: 1979–1990) temperature change and its statistical significance, as simulated by a GCM (Fig. 6a) in the altitude region of the observed lower stratospheric ozone change (tropopause to ~7 km. above), with that derived from satellite observations (Figure 6b) of the lower

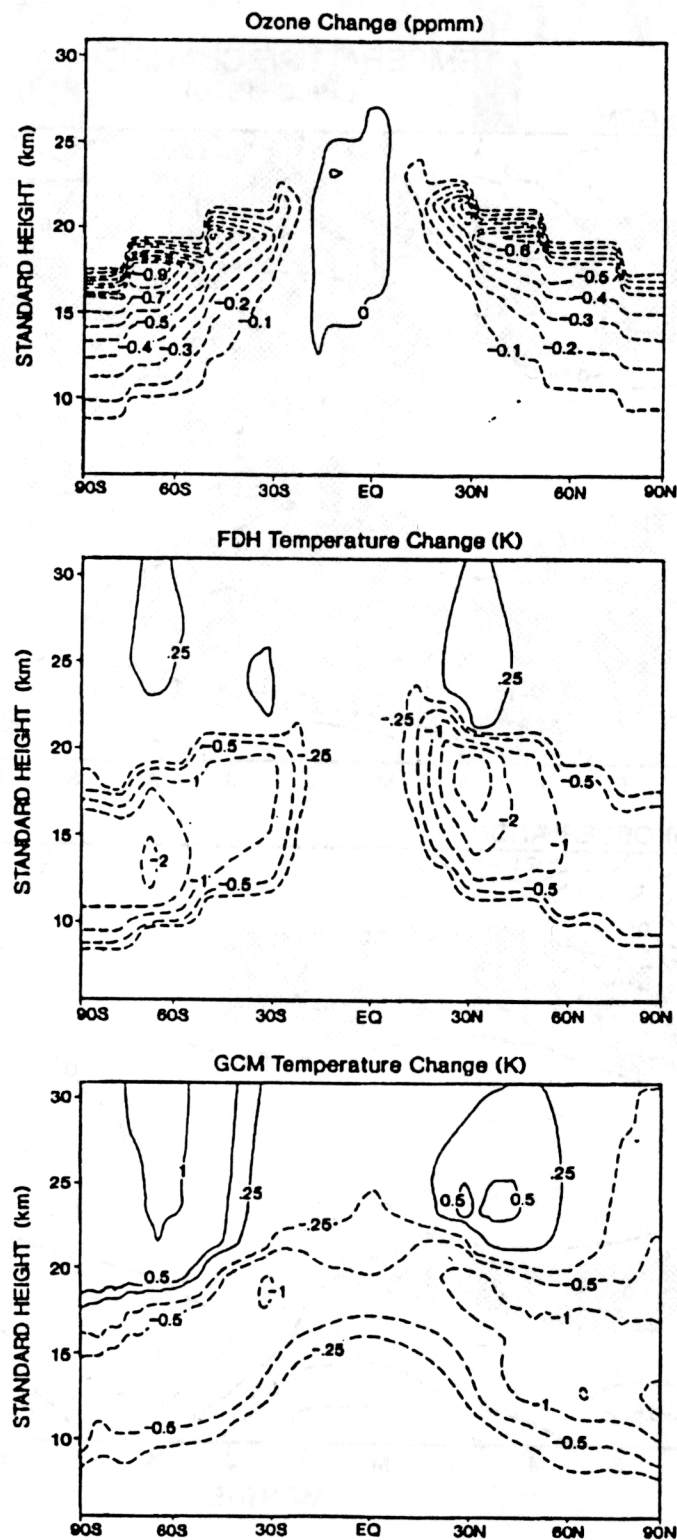


Fig. 5 Annual-mean stratospheric ozone loss profile (top panel), and the corresponding temperature changes, as obtained using a FDH model (middle panel) and GCM (bottom panel). [Adapted from the model simulations of Ramaswamy et al. (1992 and 1996)].

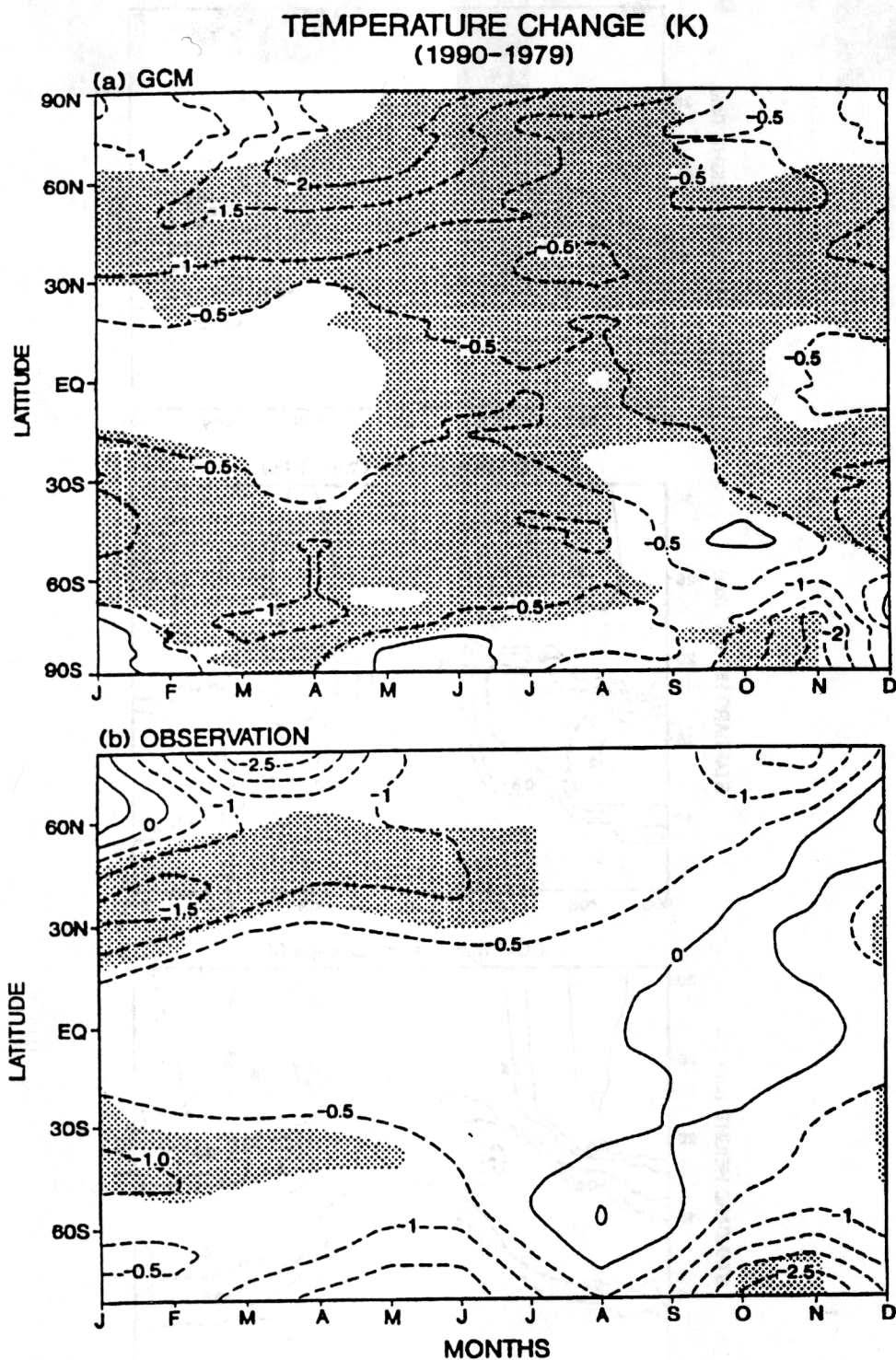


Fig. 6 Zonally-averaged, monthly mean, lower stratospheric temperature change 1979–1991: (a) as simulated by the general circulation model (90S to 90N) due to the observed global ozone depletion, and (b) as inferred (Randel and Cobb, 1994) from satellite observations (82.5S to 82.5N). Shaded areas show statistical significance at the 95% confidence level. [Reprinted by permission from *Nature* (Ramaswamy et al., *Nature*, 382, 616–618, 1996) Copyright (1996). Macmillan Magazines Ltd.].

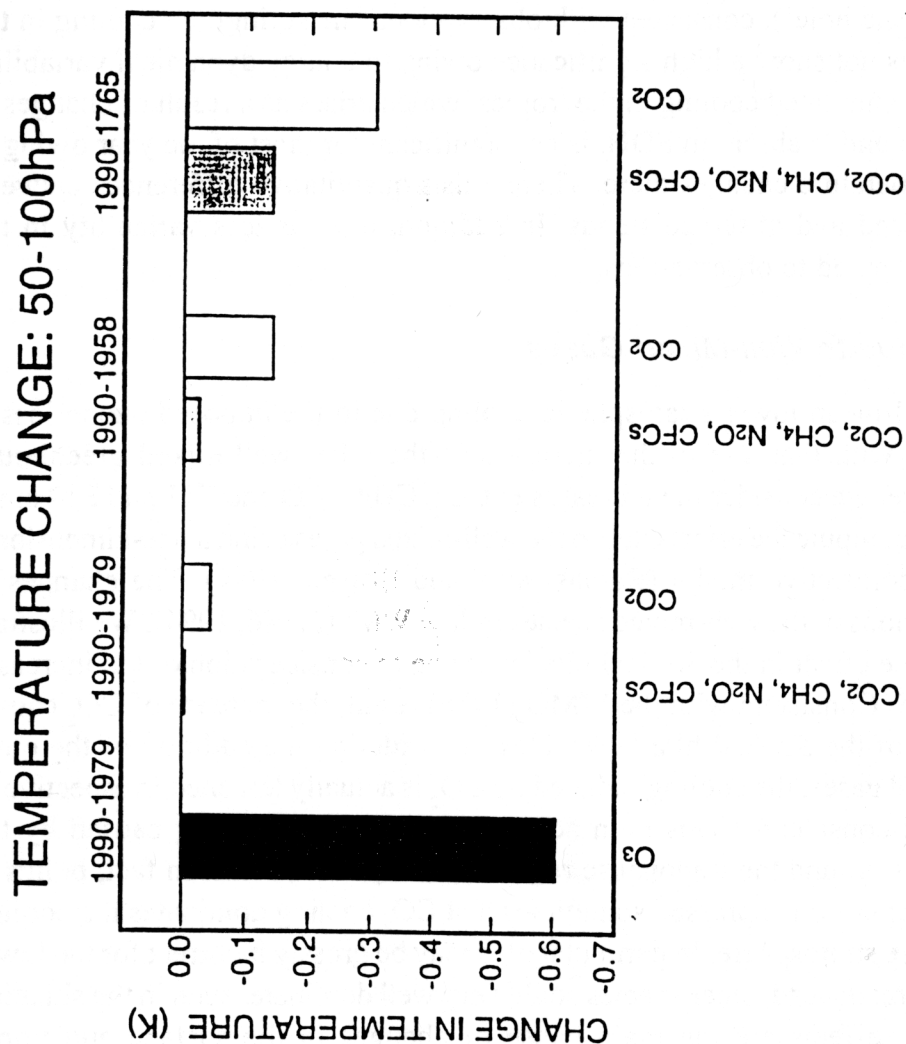


Fig. 7 Computed global- and annual-mean temperature changes in the ~50–100 hPa (~16–21 km.) lower stratospheric region. The result for the ozone depletion corresponds to the 1979 to 1990 losses, and is computed using a GCM. The results for CO₂ alone, and for all the well-mixed greenhouse gases together (viz., CO₂, CH₄, N₂O and CFCs) are computed using a 1D RCM for three different periods. [Reprinted by permission from Nature (Ramaswamy et al., Nature, 382, 616–618, 1996) Copyright (1996) Macmillan Magazines Ltd.]

stratosphere for the same period (Randel and Cobb, 1994). In the midlatitudes, both panels illustrate a cooling from ~January to October in the northern hemisphere and from ~September to July in the southern hemisphere. The cooling in the midlatitudes of the northern hemisphere from ~December to July, and in the southern hemisphere from ~December to May, are statistically significant in both model and observation. Near the poles, both the simulation and observation exhibit relatively large magnitude of cooling during winter and spring. The simulated cooling in the Antarctic is highly significant during the austral spring (period of the 'ozone hole'), consistent with observation. The springtime cooling in the Arctic does not show a high significance owing to a large dynamical variability there. The simulated cooling in the tropics, which arises as a result of changes in circulation and is absent in FDH, is not significant for most of the year owing to small temperature changes there. There exists quantitative differences between the simulated and observed trends. In addition, there is less variability in the model compared to observations.

Effects due to Well-Mixed Gases

The global-mean lower stratospheric cooling due to the imposed ozone loss is compared with that due to the increases in the other well-mixed greenhouse gases. Here, we consider the increases in CO_2 , CH_4 , N_2O and F11 and F12 since 1760. We compute the effects due to the well-mixed gases using a one-dimensional radiative-convective model (Ramaswamy and Bowen, 1994). The changes in concentrations of the well-mixed species follow WMO (1986, 1994). We illustrate in Fig. 7 the effect in the 50–100 hPa layer due to consideration of the increases since 1765. Consistent with the WMO (1986) result, the increase of CO_2 causes a cooling of the 50–100 hPa layer. Next, considering the addition of the other well-mixed gases, the cooling induced by CO_2 is actually lessened irrespective of the period considered. This is in accordance with the warming caused by the other gases around the tropopause region (WMO, 1986). This, in fact, points to a erroneous notion expressed sometimes that CO_2 cooling dominates the cooling of the entire stratosphere. In particular, this may be grossly incorrect for the lower stratosphere; instead, other species could very well dominate, even in the situation when CO_2 effects are the main cause of changes in the surface and upper stratosphere.

Next, we compare the RCM results with the GCM result for ozone. Figure 7 illustrates that the effects due to lower stratospheric ozone loss in a decade's timescale have caused more cooling there than the entire well-mixed greenhouse gases' change since the past two centuries. This is an important point inasmuch as it links the observed lower stratospheric cooling to principally ozone changes. There is another salient aspect to the comparison of ozone versus the other trace gases. This has to do with the vertical profile of temperature change observed

over the past 2–3 decades. From calculations, when the changes due to only CO₂ are compared with that due to all well-mixed gases, the transition from a warming in the troposphere to a cooling in the stratosphere occurs at a higher altitude. This is related to the fact that the non-CO₂ well-mixed gases add substantial heating in the vicinity of the tropopause, as seen in Figure 7. When the ozone changes, as computed from the GCM (e.g. Fig. 5), are considered, the height of transition is significantly lowered relative to the cases with CO₂-only or with all the well-mixed gases taken together. This is owing to the strong cooling impact of ozone loss in the lower stratosphere. The suggestion that the transition in the vertical profile from a warming to a cooling occurs at a much lower elevation than models with only CO₂ increases or effective CO₂ increases have been affirmed by the studies of Hansen *et al.* (1995) and Santer *et al.* (1996).

Attribution of Observed Temperature Trends

Lower Stratosphere

As far as the global lower stratosphere is concerned, there is now a firm documentation of the changes in ozone and well-mixed greenhouse gases. The importance of ozone depletion relative to that due to changes in other greenhouse gases that are well-mixed (CO₂, CH₄, N₂O, CFCs) have been evaluated by several studies with various types of models (1D to 3D). Miller *et al.* (1992) and Hansen *et al.* (1995) demonstrate that the global-mean lower stratospheric temperature change in the 1980s can be explained only when ozone changes are considered. Ramaswamy *et al.* (1996) show that the global, annual-mean GCM temperature change due to the decadal ozone losses in the ~50–100 hPa (~16–21 km.) lower stratospheric region is much greater than that due to increases in CO₂ only and all well-mixed greenhouse gases taken together (Figure 7). The global-mean decadal cooling in the 1980s due to ozone is estimated to be ~0.5 to 0.6K which is comparable to the reported decadal trends from observations. The well-mixed gases' effect is much smaller, less than one-fourth that due to ozone depletion. In contrast to the decadal ozone effects since ~1979, consideration of increases in CO₂ alone since 1765 yields a cooling of only ~0.3K, while inclusion of the other well-mixed gases that tend to warm the tropopause region yields only about 0.15K. Based on model-observation comparisons and the current documented evidence regarding changes in the global concentrations of radiative species, it can be stated that the observed ozone depletion is the dominant cause of the observed global-and-annual-mean cooling of the lower stratosphere over the 1980s' decade. Uncertainties arise in model simulations owing to incomplete observational knowledge of the vertical profile of global ozone loss near the tropopause, including that in the tropical areas. While more thorough altitudinal measurements of ozone loss would lead to more precise simulation of temperature change, with cooling extending to perhaps even higher altitudes (e.g. springtime southern polar

latitudes), the lower stratosphere region, taken as a whole, can be expected to cool notably given the magnitude of the ozone losses observed. As a principal conclusion from all investigations thus far, whether ozone changes are prescribed or determined self-consistently within a model, the global lower stratospheric region, especially the mid-to-high latitudes, cools in a significant manner in simulations for the decades of the 1980s and 1990s. In addition to the above, a principal feature from especially the GCM studies is the reasonably good correspondence of the zonal-mean lower stratospheric cooling trends since ~1979 with satellite and radio-sonde records (e.g. Hansen *et al.*, 1993). It is concluded that the reasonable consistency of the simulated cooling pattern and magnitudes with that observed, including the regimes of statistically significant changes, coupled with the high correlations noted between observed temperature changes and ozone losses, confirm the notion that ozone depletion has caused a substantial spatially-and-seasonally-dependent effect in the lower stratosphere over the past decade. For example, Figure 6 highlights the model-observation consistency with regard to magnitude and statistical significance in the mid-latitudes of both hemispheres during the first half of the year, and during the Antarctic springtime.

Although the attribution of the observed temperature trends to the observed ozone depletion in the lower stratosphere is strong in the global, annual-mean sense, the spatial and temporal aspects demand more circumspection. However, no other cause besides ozone depletion has been shown as yet to yield a latitude-month fingerprint such as that seen in the observations (Figure 6b). Thus, in the zonal-mean, seasonal sense, it can be stated that ozone is identified as an important causal factor of lower stratospheric temperature change.

Possible secular changes in other radiatively-active species are estimated to contribute smaller decadal effects than the stratospheric ozone loss. Information on decadal changes in global water vapor and clouds is insufficient to estimate their influence precisely; there is no information at present to suggest that their effects could be as dominant as that due to the stratospheric ozone loss. Although volcanic aerosols can have substantial impact over the 1–2 years that they are present in the lower stratosphere, their effect on the past decade's temperature trend has probably been small compared to ozone. There is little evidence to suggest that forcings from the troposphere (e.g. sea-surface temperature changes) or natural climate variability or solar cycle have significantly influenced the global lower stratospheric temperature change over the past two decades, although, in the absence of rigorous long-term observations, a precise estimate of their contributions cannot be obtained. It is noted that some ozone loss has been reported for the 1970s, too, (Lacis *et al.*, 1990) which would have contributed to the small observed cooling during that decade. However, this contribution is not likely to have been as much as in the 1980s and 1990s, since the ozone losses for the earlier decades are concluded to have been never as high as those in recent ones (Bojkov and Fioletov, 1995).

There is a scarcity of knowledge on the low frequency variability of the stratosphere and its causes—from either observations or models. Unlike surface temperature measurements which span multi-decades, those for the stratosphere are available only from about late 1950s, and the continuous record is available only at a few locations in the NH. This makes it difficult to assess accurately the low frequency variability. While global coverage has become possible with the MSU and SSU satellites since 1979, the time period available to-date is too short to assess any thing beyond inter-annual variability; certainly, rigorous decadal-scale variability analysis will not be possible until data for a few more decades become available. The model simulations to-date suggest an inter-annual variability in some features that bear some resemblance to that observed, but there are also features that the existing models either cannot reproduce or fail to mimic the observations (e.g. Hamilton *et al.*, 1995). A prominent uncertainty arises due to the lack of a proper simulation of the polar wintertime and winter-to-spring transitional temperatures (including sudden warmings) from first principles. The usual method to reproduce observations is to “tune” the model in some manner, e.g. gravity-wave drag. The quantitative effect that this has on the fidelity of the simulation of trends and variability remains to be determined.

In general, the effect of tropospheric climate change due to changes in trace gases and aerosols, equator-to-pole tropospheric temperature gradient, waves propagating into the stratosphere, and the resulting radiative-dynamical-chemical stratospheric state are not well understood in a quantitative manner. For example, different GCMs suggest substantially different manner of changes in the characteristics of the planetary wave activity due to increase of CO₂, which would, in turn, impact the radiative-dynamical interactions and the magnitude of stratospheric temperature changes (Fels *et al.*, 1980; Mahlman *et al.*, 1992; Graf *et al.*, 1995; Shindell *et al.*, 1998; Rind *et al.*, 1998).

Middle and Upper Stratosphere

Unlike the case for the lower stratosphere, the trends and significance estimated from the different observational platforms for the middle and upper stratosphere are not as robustly consistent across the different datasets. The satellite, lidar and rocket data, although having a consistency in terms of the cooling in the middle and upper stratosphere (above ~50 hPa, e.g. Figures 3 and 4), do not exhibit the same degree of coherency that exists with respect to both magnitude and statistical significance for the different datasets of the lower stratosphere (Figure 1).

In the middle and upper stratosphere, model results suggest that the increases in the well-mixed greenhouse gases and changes in ozone will contribute to temperature changes (WMO, 1999). The overall picture from the annual-mean model simulations is one of cooling from the lower to the upper stratosphere. This cooling in the middle stratosphere due to the well-mixed gases can be expected to be

enhanced by the ozone losses there; the latter is estimated to yield about a 0.3 K/decade cooling using the SAGE depletion for the 1980s period. The computed vertical profile (WMO, 1999) bears a qualitative similarity to the observations (e.g. Figures 3, 4) with regard to the cooling of the entire stratosphere. This reaffirms the secular cooling trend due to greenhouse gas changes inferred for the stratosphere from shorter records (WMO: 1990a, 1990b).

However, at altitudes above the lower stratosphere, there are major quantitative differences between the modeled and observed cooling. The simulated cooling increases with height when only the well-mixed gases are considered (WMO, 1999) whereas the observations indicate a rather uniform trend between 20–35 km. (with perhaps even a slight reduction at ~30–35 km.; *see* Figures 3,4). Additionally, the magnitude of the modeled cooling in the upper stratosphere is less than that observed (WMO, 1999), e.g. at ~45 km., the modeled cooling is about 1 K/decade due to the well-mixed greenhouse gases and about 0.3K/decade due to ozone, while the observed cooling is greater than 1.5K/decade (e.g. at 45 km. In Figures 3, 4). Some of this bias could be due to water vapor whose decadal trend in the 1980s globally is not known. Recent satellite data suggests an upward trend over the past five years which would add to the cooling trend computed for the upper stratosphere and reduce the present discrepancy.

The vertical and latitudinal magnitude of the cooling, and likewise the location of the warming region above the cooling in the lower stratosphere (*see* Fig. 5), are very sensitive to the vertical profile of ozone depletion imposed in the model. The models invariably locate the cooling at exactly the region of the imposed ozone loss, with a warming immediately above it at the higher latitudes. Thus, any shift of the altitude extent of ozone depletion in the model has the potential to shift the peak cooling, and thus alter the vertical profile of the computed cooling trend. In turn, this affects the quantitative inferences about the consistency between computed and observed temperature trends in the middle and upper stratosphere.

Concluding Remarks

There is a strong need for a continuous temperature trends analyses and assessment, with research findings made available at frequent intervals (e.g. every 5 years). These should include up dates and quality control of datasets, model-observation comparisons, detection and attribution analyses, and improved estimates for the future based on scenarios of potential changes in atmospheric composition. Broadly speaking, the tasks include a systematic analyses of the quality and accuracy of all of the instrumental data, quantitative analyses of the spatial and temporal variations manifest in the observational data, improvements in model simulations and the understanding of 'natural' or unforced variability, model responses to changes in composition that occur within the stratosphere and also that in the troposphere (to the extent that they affect the stratosphere),

and careful diagnoses of the trends and their attribution using observations and model simulations. Since the scope of the subject is necessarily large and global in nature, it would be beneficial for the overall monitoring and research to be performed in close coordination with appropriate national and international scientific bodies (e.g. WCRP/ SPARC, WMO, COSPAR, IAGA etc.). It is also vital to sustain a linkage between temperature trends activities and the monitoring of the concentrations of radiatively active species, especially those that are temporally and spatially variable (e.g. ozone, water vapor and aerosols).

Acknowledgments

I thank M. D. Schwarzkopf for a number of fruitful conversations on this subject. I am grateful to the members of the SPARC-STTA group and to the authors of the WMO (1999) Chapter 5 for their invaluable suggestions and comments on various aspects of stratospheric temperature trends.

References

1. Angell, J. K., The close relation between Antarctic total-ozone depletion and cooling of the Antarctic low stratosphere, *Geophys. Res. Lett.*, 13, 1240–1243, 1986.
2. Bailey, M. J., A. O'Neill, and V. D. Pope, Stratospheric analyses produced by the United Kingdom Meteorological Office, *J. Appl. Meteor.*, 32, 9, 1472–1483, 1993.
3. Bojkov, R. and V. E. Fioletov, Estimating the global ozone characteristics during the last 30 years, *J. Geophys. Res.*, 100, 16537–16551, 1995.
4. Christy, J. R., R. W. Spencer and R. T. McNider, Reducing noise in the daily MSU lower tropospheric temperature dataset, *J. Climate*, 8, 888–896, 1995.
5. Dunkerton, T., D. Delisi and M. Baldwin, Examination of middle atmosphere cooling trend in historical rocketsonde data, *Geophys. Res. Lett.*, submitted, 1998.
6. Fels, S.B. and L.D. Kaplan, A test of the role of longwave radiative transfer in a general circulation model, *J. Atmos. Sci.*, 33, 779–789, 1975.
7. Fels, S. B., J. D. Mahlman, M. D. Schwarzkopf, and R. W. Sinclair, Stratospheric sensitivity to perturbations in ozone and carbon dioxide: Radiative and dynamical response, *J. Atmos. Sci.*, 37, 2265–2297, 1980.
8. Finger, F.G., M.E. Gelman, J.D. Wild, M.L. Chanin, A. Hauchecorne, and A.J. Miller, Evaluation of NMC upper-stratospheric temperature analyses using rocketsonde and lidar data, *Bull. Am. Meteorol. Soc.*, 74, 789–799, 1993.
9. Gelman, M.E., A.J. Miller, K.W. Johnson and R.M. Nagatani, Detection of long-term trends in global stratospheric temperature from NMC analyses derived from NOAA satellite data, *Adv. Space. Res.*, 6, 17–26, 1986.
10. Gelman, M. E., A. J. Miller, R. N. Nagatani and C. S. Long, Use of UARS data in the NOAA stratospheric monitoring program, *Adv. Space Res.*, 14, 9(21)–9(31), 1994.
11. Gille, S. T., A. Hauchecorne and M-L. Chanin, Semidiurnal and diurnal tide effects in the middle atmosphere as seen by Rayleigh lidar, *J. Geophys. Res.*, 96, 7579–7587, 1991.

12. Golitsyn, G. S., A. I. Semenov, N. N. Shefov, L. M. Fishkova, E. V. Lysenko and S. P. Perov, Long-term temperature trends in the middle and upper atmosphere, *Geophys. Res. Lett.*, 23, 1741–1744, 1996.
13. Goody, R. and Y. Yung, Atmospheric Radiation, *Oxford University Press*, Chapter 9, 1988.
14. Graf, H-F., J. Perlwitz, I. Kirchner and I. Schult, Recent northern winter climate trends, ozone changes and increased greenhouse gas forcing, *Contrib. Atm. Phys.*, 68, 233–248, 1995.
15. Hamilton, K., R. J. Wilson, J. D. Mahlman and L. J. Umscheid, Climatology of the GFDL SKYHI troposphere-stratosphere-mesosphere general circulation model, *J. Atmos. Sci.*, 52, 5–43, 1995.
16. Hansen, J., A. Lacis, R. Ruedy, M. Sato, and H. Wilson, How sensitive is the world's climate? *Natl. Geogr. Res. Explor.*, 9, 142–158, 1993.
17. Hansen, J. E., H. Wilson, M. Sato, R. Ruedy, K. Shah and E. Hansen, Satellite and surface temperature data at odds? *Clim. Change*, 30, 103–117, 1995.
18. Hansen, J., M. Sato, R. Ruedy, A. Lacis, K. Asamoah, K. Beckford, S. Borenstein, E. Brown, B. Cairns, B. Carlson, B. Curran, S. de Castro, L. Druyan, P. Etwarrow, T. Ferede, M. Fox, D. Gaffen, J. Glascoe, H. Gordon, S. Hollandsworth, X. Jiang, C. Johnson, N. Lawrence, J. Lean, J. Lerner, K. Lo, J. Logan, A. Luckett, M. P. McCormick, R. McPeters, R. Miller, P. Minnis, I. Rambaran, G. Russell, P. Russell, P. Stone, I. Tegen, S. Thomas, L. Thomason, A. Thompson, J. Wilder, R. Willson and J. Zawodny, Forcings and chaos in interannual to decadal climate change, *J. Geophys. Res.*, 102, 25679–25720, 1997b.
19. Hauchecorne, A., M-L. Chanin and P. Keckhut, Climatology and trends of the middle atmospheric temperature (33–87 km.) as seen by Rayleigh lidar over the south of France, *J. Geophys. Res.*, 96, 15297–15309, 1991.
20. Kalnay, E. *et al.*, The NCEP/NCAR 40-year reanalysis project, *Bull. Amer. Met. Soc.*, 77, 3, 437–471, 1996.
21. Keckhut, P., A. Hauchecorne and M.L. Chanin, Midlatitude long-term variability of the middle atmosphere: Trends and cyclic and episodic changes, *J. Geophys. Res.*, 100, 18887–18897, 1995.
22. Keckhut, P., M. E. Gelman, J. D. Wild, F. Tissot, A. J. Miller, A. Hauchecorne, M-L. Chanin, E. F. Fishbein, J. Gille, J. M. Russell III, and F. W. Taylor, Semidiurnal and diurnal temperature tides (30–55 km): Climatology and effect on UARS lidar data comparisons, *J. Geophys. Res.*, 101, 10299–10310, 1996.
23. Keckhut P., F.J. Schmidlin, A. Hauchecorne and M.-L. Chanin, Trend estimates from rocketsondes at low latitude station (8S–34N), taking into account instrumental changes and natural variability, *J. Atm. Solar-Terr. Phys.*, 61, 447–459, 1999.
24. Kiehl, J.T., B.A. Boville, and B.P. Riegler, Response of a general circulation model to a prescribed Antarctic ozone hole, *Nature*, 332, 501–504, 1988.
25. Kokin, G., and E. Lysenko, On temperature trends of the atmosphere from rocket and radiosonde data, *J. Atmos. Terr. Phys.*, 56, 1035–1044, 1994.
26. Komuro, H., Long-term cooling in the stratosphere observed by aerological rockets at Ryori, Japan, *Met. Soc. of Japan*, 1081–1082, 1989.
27. Koshelkov, Yu. P. and G. R. Zakharov, On temperature trends in the Arctic lower stratosphere, *Meteorologia i Gidrologia*, 5, 45–54, 1998.

28. Labitzke, K. and H. van Loon, Trends of temperature and geopotential height between 100 and 10 hPa in the Northern Hemisphere, *J. Meteor. Soc. of Japan*, 72, 5, 643–652, 1994.
29. Labitzke, K., and H. van Loon, A note on the distribution of trends below 10hPa: The extratropical northern hemisphere. *J. Meteor. Soc. Japan*, 73, 883–889, 1995.
30. Lacis, A.A., D.J. Wuebbles, and J.A. Logan, Radiative forcing of climate by changes in the vertical distribution of ozone, *J. Geophys. Res.*, 95, 9971–9981, 1990.
31. Lysenko, E. V., G. Nelidova and A. Prostova, Changes in the stratospheric and mesospheric thermal conditions during the last 3 decades: 1. The evolution of a temperature trend, *Izvestia, Atmosph. Oceanic Physics*, 33, 2, 218–225, 1997.
32. Mahlman, J. D., A looming Arctic ozone hole? *Nature*, 360, 209, 1992.
33. Mahlman, J.D., J.P. Pinto, and L.J. Umscheid, Transport, radiative, and dynamical effects of the antarctic ozone hole: a GFDL “SKYHI” model experiment, *J. Atmos. Sci.*, 51, 489–508, 1994.
34. Miller, A.J., R.M. Nagatani, G.C. Tiao, X.F. Niu, G.C. Reinsel, D. Wuebbles, and K. Grant, Comparisons of observed ozone and temperature trends in the lower stratosphere. *Geophys. Res. Lett.*, 19, 929–932, 1992.
35. Nash, J., and G. F. Forrester, Long-term monitoring of stratospheric temperature trends using radiance measurements obtained by the TIROS-N series of NOAA spacecraft, *Adv. Space Res.*, 6, 37–44, 1986.
36. Oort, A.H., and H. Liu, Upper-air temperature trends over the globe, 1956–1989. *J. Climate*, 6, 292–307, 1993.
37. Parker, D.E., and D.I. Cox, Towards a consistent global climatological rawinsonde database, *Intl. J. Climatology*, 15, 473–496, 1995.
38. Parker, D. E., M. Gordon, D. P. N. Cullum, D. M. H. Sexton, C. K. Folland and N. Rayner, A new global gridded radiosonde temperature data base and recalculated temperature trends, *Geophys. Res. Lett.*, 24, 1499–1502, 1997.
39. Ramanathan, V. and R.E. Dickinson, The role of stratospheric ozone in the zonal and seasonal radiative energy balance of the Earth-troposphere system. *J. Atmos. Sci.*, 36, 1084–1104, 1979.
40. Ramaswamy, V. and M.M. Bowen, Effect of changes in radiatively active species upon the lower stratospheric temperatures. *J. Geophys. Res.*, 99, 18909–18921, 1994.
41. Ramaswamy, V., M. D. Schwarzkopf and W. Randel, Fingerprint of ozone depletion in the spatial and temporal pattern of recent lower-stratospheric cooling. *Nature*, 382, 616–618, 1996.
42. Ramaswamy, V., M.D. Schwarzkopf, and K.P. Shine, Radiative forcing of climate from halocarbons-induced global stratospheric ozone loss, *Nature*, 355, 810–812, 1992.
43. Randel, W. J., The anomalous circulation in the Southern hemisphere stratosphere during spring 1987, *Geophys. Res. Lett.*, 15, 911–914, 1988.
44. Randel, W.J., and J.B. Cobb, Coherent variations of monthly mean total ozone and lower stratospheric temperature, *J. Geophys. Res.*, 99, 5433–5447, 1994.
45. Rind, D. D. Shindell, P. Lonergan, and N. K. Balachandran, Climate change and the middle atmosphere. Part III: The doubled CO₂ climate revisited, *J. Clim.*, in press, 1998.
46. Santer, B. D., K. E. Taylor, T. M. L. Wigley, T. C. Johns, P. D. Jones, D. J. Karoly, J. F. B. Mitchell, A. H. Oort, J. E. Penner, V. Ramaswamy, M. D. Schwarzkopf, R. J. Stouffer and S. Tett, A search for human influences on the thermal structure of the atmosphere, *Nature*, 382, 39–46, 1996.

47. Santer, B. D., J. J. Hnilo, T. M. L. Wigley, J. S. Boyle, C. Doutriaux, M. Fiorino, D. E. Parker and K. E. Taylor, Uncertainties in 'Observational' estimates of temperature change in the free atmosphere, *J. Geophys. Res.*, submitted, 1998.
48. Schubert, S. R., R. Rood and J. Pfaendtner, An assimilated dataset for earth science applications, *Bull. Amer. Met. Soc.*, 74, 2331–2342, 1993.
49. Shindell, D. T., D. Rind, and P. Lonergan, Increased polar stratospheric ozone losses and delayed eventual recovery owing to increasing greenhouse-gas concentrations, *Nature*, 392, 598–592, 1998.
50. Spencer, R. W. and J. R. Christy, Precision lower stratospheric temperature monitoring with the MSU technique, validation and results 1979–1991, *J. Climate*, 6, 1194–1204, 1993.
51. WMO Atmospheric Ozone:1985, Global Ozone Research and Monitoring Project Rep. No. 16, Chapter 15, 1986.
52. WMO Report of the International Ozone Trends Panel: 1988, Global Ozone Research and Monitoring Project Report No. 18, Chapter 6, Geneva, 1990a.
53. WMO Scientific Assessment of Stratospheric Ozone:1989, Global Ozone Research and Monitoring Project—Report No. 20, Chapters 1 and 2, Geneva, 1990b.
54. WMO Scientific Assessment of Ozone Depletion:1991, Global Ozone Research and Monitoring Project—Report No. 25, Chapters 2 and 7, Geneva, 1992.
55. WMO Scientific Assessment of Ozone Depletion:1994, World Meteorological Organization Global Ozone Research and Monitoring, Project Report No. 37, Chapter 8, Geneva, 1995.
56. WMO Scientific Assessment of Ozone Depletion:1998, World Meteorological Organization Global Ozone Research and Monitoring, Project Report No. 44, Geneva, 1999.